

POWER LOSSES ESTIMATION FOR VISUALIZATION OF HEAT DISTRIBUTION

Patrik RESUTIK, Slavomir KASCAK

Department of Mechatronics and Electronics, Faculty of Electrical Engineering and Information Technology, University of Zilina, 010 26 Zilina, Slovak Republic

patrik.resutik@feit.uniza.sk, slavomir.kascak@feit.uniza.sk

DOI: 10.15598/aeec.v18i3.3764

Abstract. For designing power electronics, especially high-power-density systems, power loss estimation is a very important step in the design process. The estimation of losses without using a mathematical method, but instead using a simulation approach can significantly lower design time. In this paper, the estimation of the power losses by the simulation method using MATLAB Simulink is presented. The main goal of this paper is the estimation of the worst-case scenario of the inverter losses powering the three-phase asynchronous motor. Simulation is using real parameters of the used semiconductors to accurately estimate power losses. The simulation model consists of two main parts. The first one calculates power losses in semiconductors based on the provided parameters and his temperature. The second part calculates the temperature of the system based on the cooling model and losses calculated by the first system. Results in the form of the losses are used in the Fusion 360 software to simulate the temperature distribution of the heatsink. This simulation is supported by the calculation of the convection coefficient of the heatsink in different airflows. Additionally, two types of heat transfer were simulated, convection only and convection plus radiation type of heat dissipation.

Keywords

Heat distribution, IGBT, inverter, MATLAB, power losses.

1. Introduction

Innovation in the field of power electronics leads to a significant reduction of the power device dimensions. This results in much higher heat flux generated by

semiconductors. For ensuring the reliability and performance of the design, the recommended junction temperature of the semiconductor cannot be exceeded. Therefore, electrical and thermal modeling is of great interest to ensure the proper function of the device [1], [2], [3] and [4]. There is a lot of options to estimate power losses generated by power semiconductor, from which can be chosen.

The first direct calculation can be used, involving RMS and AV values of voltage and current. By this method, all types of power losses can be estimated [5]. Secondly, the indirect calculation of the losses using instantaneous values of the voltage and current can be used [6]. For better estimations, static and dynamic models of the used switch can be used to accurately estimate power losses. The precision of this result depending on the accuracy of the used model [7]. Another approach can be selected using a finite element approach to estimate temperature and flux distribution [8], [9] and [10]. Finally, the experimental measurement can be used to estimate losses and cooling, but this requires a physical sample of the design [11] and [12].

Many publications use only equations or only the static parameters of the used semiconductor. In [13], the forward voltage curve of the IGBT and diode is linearized. This linearized formula is used to calculate conducting power losses. In [14], energies for the switching losses are scaled to the target application using the values from datasheet given by manufacturer and values given by the target application. In [15] and [16], the authors calculate the dynamic resistance of the diode and IGBT from the datasheet curves. Average and RMS values of current are estimated, and losses are calculated by the well-known formula $P = V_F \cdot I_{AVG} + R_D \cdot I_{RMS}$, where V_F and R_D are the forward voltage and dynamic resistance, respectively. These methods are not suitable for the dynamic

system analysis, for example, in the step change of the load current. In this publication, instantaneous values of the collector current I_C and collector-emitter voltage V_{CE} are used for conductive losses calculation. For switching losses, instantaneous values of turn-on and turn-off switching losses are used. For heat dissipation, the thermal model is created in the next step. This model uses values of thermal resistance of the IGBT device from the manufacturer's datasheet, and the value of thermal resistance of the used heatsink. In MATLAB-Simulink, these two models are fused. The output of the electrical model, which is the total power loss of the device, is fed into the thermal model. The thermal model uses this value of power loss to calculate the temperature of the components presented in the thermal model. The output of the thermal model is fed back to the electrical model, so the simulation could use actual temperature for losses calculation because parameters of the semiconductor switch are temperature dependent. Finally, the average steady-state losses produced by MATLAB-Simulink simulation is used in the next software. For the heat distribution with considering convection and radiation, the software Fusion 360 is used.

This paper focuses on electro-thermal simulation in three-phase inverters based on IGBT semiconductor switches. It should be noted that the presented electro-thermal model can be used for any converter topology and transistor. The results of all the simulations and calculations are in this paper.

2. Loss Estimation Using MATLAB Simulink

For loss estimation in the three-phase inverter, the electro-thermal model in MATLAB-Simulink was created. The main part of the model is a three-phase inverter build from IGBT semiconductors. For controlling inverter and generating proper firing pulses, Field Oriented Control (FOC) is used. For load, induction motor fed by this inverter is considered. For loss calculation, characteristics of used semiconductors were added to the switch model. Included characteristics are collector current as a function of saturation voltage and temperature $I_C = f(V_{Tce}, T)$, and switching losses vs. collector current and temperature, $E_{OFF} = f(I_C, T)$ and $E_{ON} = f(I_C, T)$. For the body diode losses, characteristic of forward voltage vs forward current and temperature $I_F = f(V_{Df}, T)$ involving recovery losses was used. All characteristics consist of two curves for different temperatures, in this case, for 25 °C and 175 °C. Different temperatures can be used too, depending on manufacturer specifications. Losses generated by this model are used by the thermal model.

The classical model of the IGBT transistor is represented by the resistor substitution. So, when the transistor is on, the model is represented by the on-resistance, and when the IGBT is turned off, the model is represented by the snubber resistance and snubber capacitance. This is a basic Simulink IGBT model from the library powerlib. From the measured values of the current and the voltage, basic look-up tables are used to estimate the turn-on/turn-off energies with consideration of the temperature too. Look-up tables are generated from the provided data from the datasheet shown in Fig. 2.

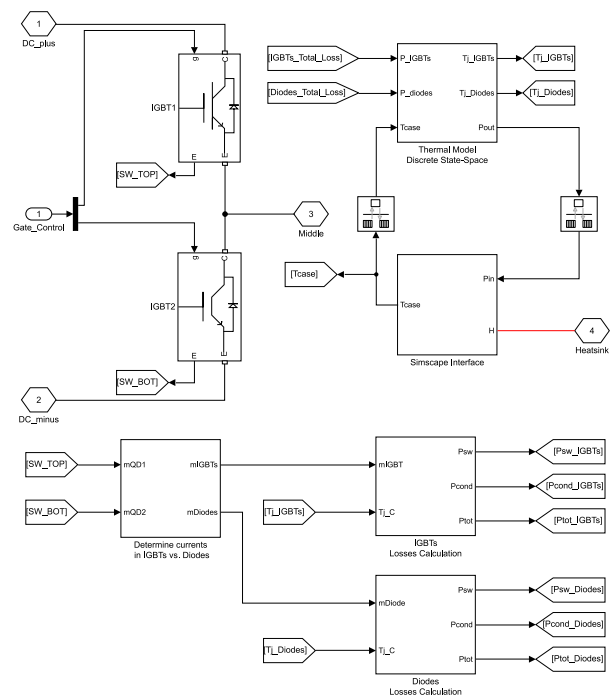


Fig. 1: Simulink model of the IGBT power loss calculation.

The thermal model uses thermal resistance of the heatsink and heat-conducting pad to estimate the temperature at different parts of the model, as junction, case, and heatsink. The value of the actual junction temperature is fed back to the electrical model, as shown in Fig. 1, where it is used to estimate turn on and turn off energies and forward voltages of IGBT and internal diode from previously mentioned characteristics. This inverter will be powering the induction motor for simulation of electric vehicle movement. Because of the character of the induction motor and the fact that the motor is variable load and can be operated at different speeds and different loads, a crucial step to investigate power losses in the inverter is determine in what conditions power losses are highest. The heatsink of the device must be designed for the worst-case scenario of the inverter operation. For this purpose, the parametric simulation was created.

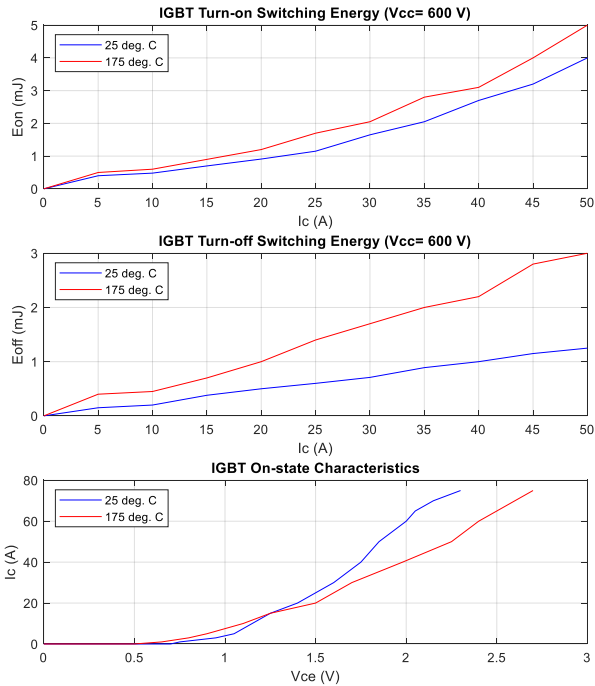


Fig. 2: IGBT data used in the simulation.

At this point, it should be noted that the operation of the electric motor at lower frequencies is less efficient. Even the operation of an electric vehicle in the city is not at speed around zero but runs at one-third of the nominal speed, except the start of the car. The parameters for simulation were the speed of the motor and load torque. Therefore, the motor speed values (1400 1250 1000 750 500) RPM and the torque values (10 20 30 40 50) Nm were chosen.

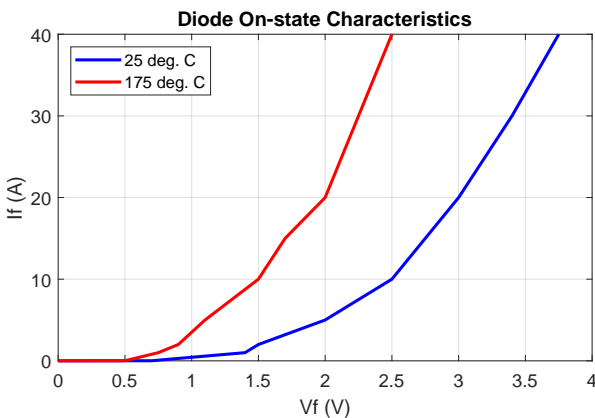


Fig. 3: Diode data used in this simulation.

In total, 25 simulations must be performed to gather all necessary data. MATLAB script was written, containing two loops, one loop is for speed selection and the second for the torque selection. Then, parametric simulation is running through the command line automatically.

When the simulation model in Simulink is started, the motor is running at speed defined by the script. After two seconds, the load is attached to the shaft of the motor. When all monitored values reach the steady-state, the mean value is gathered from the last 10000 samples. All monitored data are stored in the array variables. Then, a new simulation with new parameters is started, and the process is repeating.

After the process is finished, results from simulations are analyzed. The most important are the steady-state inverter losses in Fig. 4.

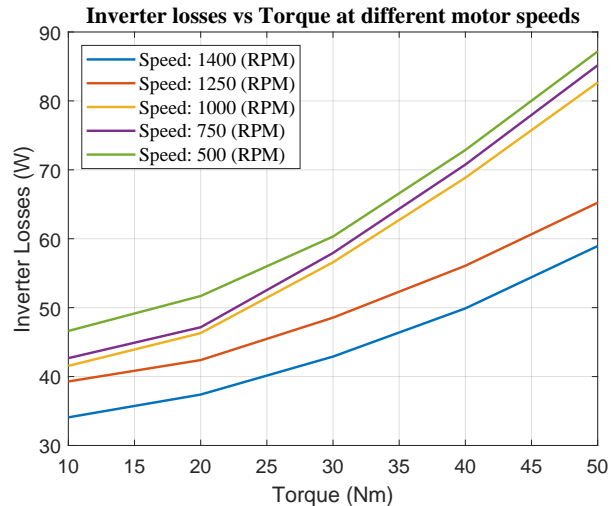


Fig. 4: Simulated power losses of the inverter.

As expected, the results show that power losses of the inverter are not highest at nominal speed and nominal torque, but at the lowest simulated speed and maximum torque. Power losses at lower speeds are higher because of lower back EMF of the motor and higher current at full torque. Because of that, the heatsink must be designed for the worst-case scenario. In this case, the power loss is about 87 W.

In the thermal model, a heatsink with a thermal resistance of $0.65 \text{ }^\circ\text{C}\cdot\text{W}^{-1}$ was used. This value of thermal resistance was measured at real heatsink with the use of power resistors. The power resistors were simulating power losses from transistors. The heatsink was closed to the enclosure to avoid airflow and maintain uniform conditions. Resistors were powered by the known current to generate known power losses. Multiple temperature sensors were mounted to monitor the temperature of the heatsink at different points. When the steady-state is reached, the thermal resistance of the heatsink is calculated by the following formula:

$$R_{ha} = \frac{T_h - T_a}{P_{TOT}}, \tag{1}$$

where R_{ha} represents heatsink thermal resistance, T_h and T_a are the heatsink and ambient temperature, respectively. Finally, P_{TOT} represents power losses.

In Fig. 5, the heatsink temperature of the inverter at different speeds and torque is shown. All values are shown for heatsink thermal resistance $0.65 \text{ }^\circ\text{C}\cdot\text{W}^{-1}$. This is the value with no airflow around the heatsink.

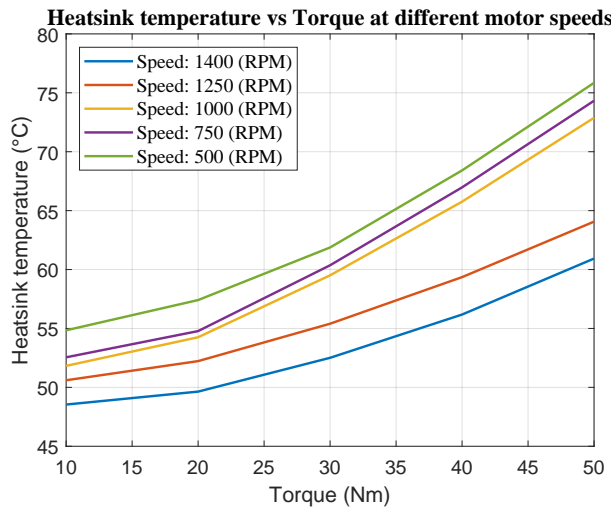


Fig. 5: Simulated temperature of the heatsink.

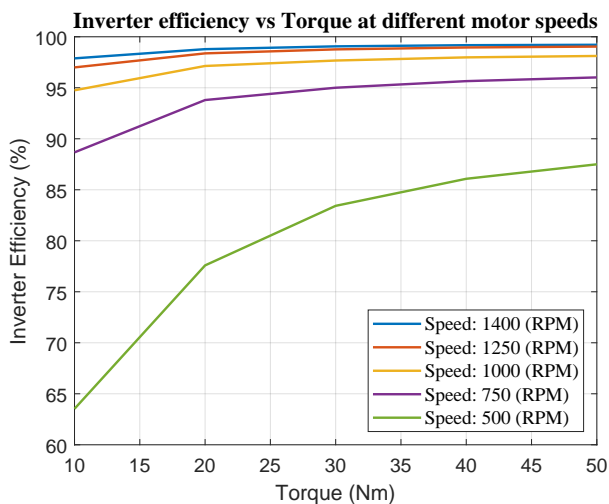


Fig. 6: Simulated inverter efficiency.

From simulation data, the efficiency of the inverter can be calculated too. The results of the simulation for the inverter efficiency can be seen in Fig. 6.

The efficiency of the inverter is lowest at the lowest speed and lowest torque. The losses are quite high, but inverter output power is low, which means low efficiency of the inverter about 64 % at this condition. The highest efficiency is at speed 1400 RPM and shaft torque 50 Nm. This means output motor power approximately 7400 W and inverter efficiency about 99.2 %.

The values of the temperatures at different points of the system from the thermal simulation were gathered too. In Fig. 7, the temperatures at different points of

the system can be seen. The exponential rise of the temperature is given by the thermal capacitance of the heatsink. This simulation was made at 500 RPM and 50 Nm load because of the highest power losses.

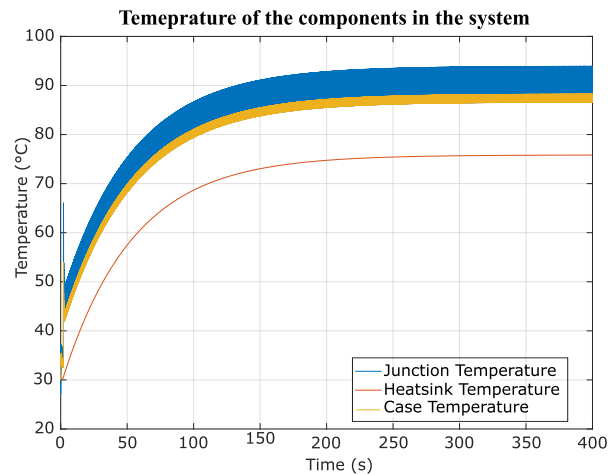


Fig. 7: Temperatures from the simulation at 500 RPM and 50 Nm.

The steady-state temperature of the heatsink is $76 \text{ }^\circ\text{C}$, the junction temperature oscillates around $90 \text{ }^\circ\text{C}$, and the case temperature around $88 \text{ }^\circ\text{C}$. The oscillation is caused by the thermal capacity of the used transistor.

3. Heat Distribution Simulation Using the Fusion 360

Recently, a new feature was added to the Fusion 360 3D modeling software. This function can calculate and simulate temperature and heat flux distribution in drawn 3D models. The first step is to draw a model of the used heatsink in the sketch mode. Another part that needs to be drawn is the IGBT model. For this, we choose the three-part model, case, junction, and backplate as different parts. This leads to a better determination of the heat spreading through the component. When all parts are modeled, they are joined to the one final model used in the thermal simulation shown in Fig. 8.

For this simulation, the next step is the material definition. Materials need to be defined for each component. The program offers a wide range of used materials. The material has defined all necessary properties needed for the simulation. For the heatsink, aluminum material was chosen. IGBT case was defined as epoxy resin and the IGBT junction and heatsink as copper. This definition is made based on [17], where copper leads to similar features as the IGBT construction.

The next step is the definition of the places and areas where heat is generated and where it is dissipated in the simulated system. The junction of each modeled IGBT was set as an internal heat source with a value of 14.5 W. This is a place where heat is generated in the simulated system. Next, areas where heat can be dissipated are defined. The area of the heatsink is a place where heat can be dissipated to the surrounding air, and in this place, convection heat transfer occurs. For this constant, different values can be selected based on material temperature and airflow around heatsink ribs. For no airflow, the value of convection was calculated with the use of [18].

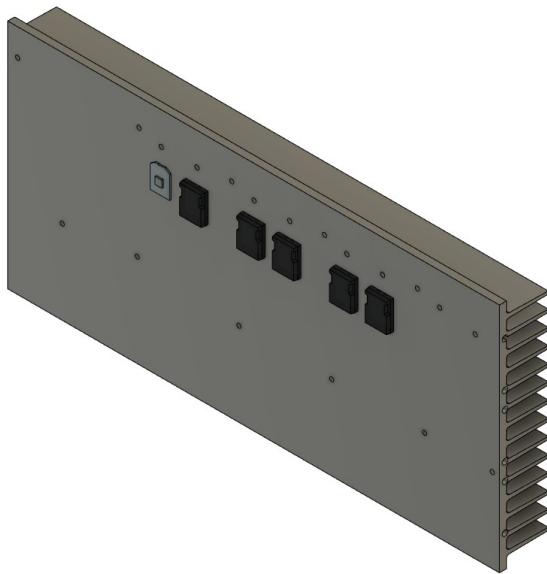


Fig. 8: Fusion 360 3D model of the heatsink and IGBT structure.

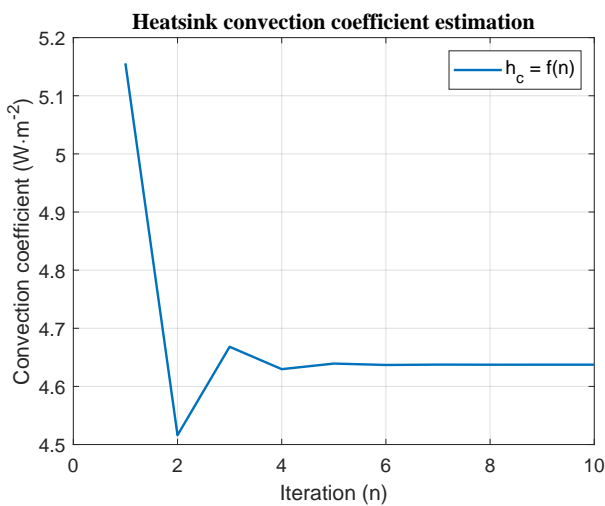


Fig. 9: The result from the convection coefficient estimation.

This document uses the physical dimensions of the heatsink to estimate the value of the convection. This

method is iterative, so the script in MATLAB was written. In total, ten iterations were performed to precisely estimate heatsink convection value. A graph of the convection value as a function of iteration can be seen in Fig. 9.

Based on this estimation, the value of $4.64 W \cdot m^{-2}$. K was used as convection value for the Fusion 360 simulation. The iteration method is capable of temperature calculation too. In the first step, the heatsink temperature is estimated. With this temperature, the Nusselt number is calculated. With Nusselt number known, convection value and new heatsink temperature are calculated. Then, with a new heatsink temperature, the Nusselt number is recalculated again. These steps are made until the result is a steady-state number. The result of calculated heatsink temperature using the iterative method can be seen in Fig. 10.

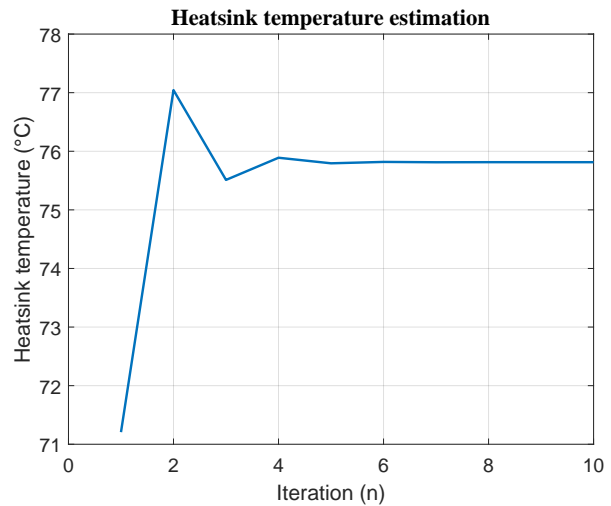


Fig. 10: Heatsink temperature calculated by the iteration method.

It is important to remember, this estimation considering only convection heat transfer from the heatsink to air. So, the simulation in Fusion was made only with convection transfer too. The results can be seen in Fig. 11.

The average heatsink temperature was estimated to be $75.8^{\circ}C$. The program offers point probe placing to investigate temperature at different places at the heatsink. For further investigation, another type of heat transfer was used. The emissivity coefficient for the heatsink and IGBT case was used based on well-known values for materials. For the shiny aluminum emissivity coefficient, 0.08 was used. IGBT case is usually made from black epoxy, so the emissivity coefficient was set to 0.98. With another type of heat transfer, the simulation was run again, and the results can be seen in Fig. 12.

As can be seen, temperatures at the heatsink surface drop. The average temperature of the heatsink was estimated to be 69.4 °C.

The value of the convection coefficient is airflow dependent too. If forced air circulation needs to be simulated and investigated, the value of the convection must be adjusted accordingly.

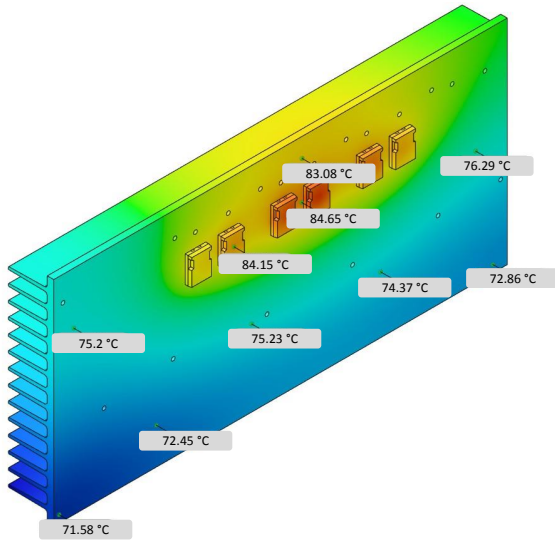


Fig. 11: The result from the simulation using only convection heat transfer.

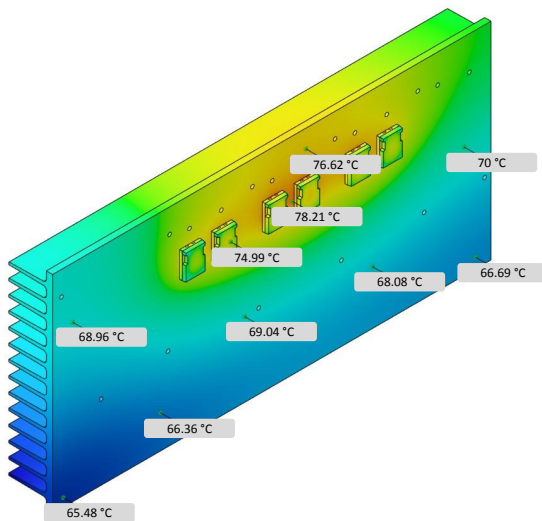


Fig. 12: The result from the simulation using convection and radiation heat transfer.

4. Heat Transfer Coefficient Estimation with Airflow

With the use of [19] and [20] based on heatsink dimensions and air constants, convection constant can

be calculated. Derived formula from [19] for Nusselt number N_u was used:

$$N_u = \left[\frac{1}{\left(\frac{R_{eb} \cdot P_r}{2} \right)^3} + \frac{1}{\left(0.664 \cdot \sqrt{R_{eb}} \cdot P_r^{0.33} \cdot \sqrt{1 + \frac{3.65}{\sqrt{R_{eb}}}} \right)^3} \right]^{-0.33}, \quad (2)$$

where P_r represents Prandtl number, and R_{eb} represents the modified channel Reynolds number calculated as:

$$R_{eb} = \frac{U \cdot b}{\nu} \cdot \frac{b}{L}, \quad (3)$$

where U represents air velocity, b is the heatsink channel width, ν is the kinematic viscosity of the air, and L represents heatsink length. In Eq. (2), Prandtl number P_r is calculated as:

$$P_r = \frac{\mu \cdot C_p}{k}, \quad (4)$$

where μ represents dynamic viscosity of the air, C_p is the specific heat of the air, and k is the thermal conductivity of the air. With all these equations, the script was created in MATLAB to calculate the dependency of the heat transfer coefficient at air velocity. The heat transfer coefficient is calculated based on the Nusselt number calculated in Eq. (2) as:

$$h = N_u \cdot \frac{k}{b}, \quad (5)$$

where N_u represents a Nusselt number calculated in Eq. (2), k represents thermal conductivity of the air, and b is the heatsink channel width. The results of the calculations can be seen in Fig. 13.

These calculated values can be used in the Fusion 360 to visualize heat spreading in the heatsink at different air velocity. When the thermal resistance of the heatsink from Eq. (5) is known, temperature can be calculated too. The result is in Fig. 14.

The value from Fig. 14 and visualization from Fig. 15 shows a good correlation between the calculated and simulated temperature by considering the value of air velocity 1 m·s⁻¹. An average simulated temperature at the heatsink, considering only convection, is shown in Fig. 15. The average temperature of the heatsink is 54.8 °C. On the other side, the temperature, considering also radiation, is depicted in Fig. 16.

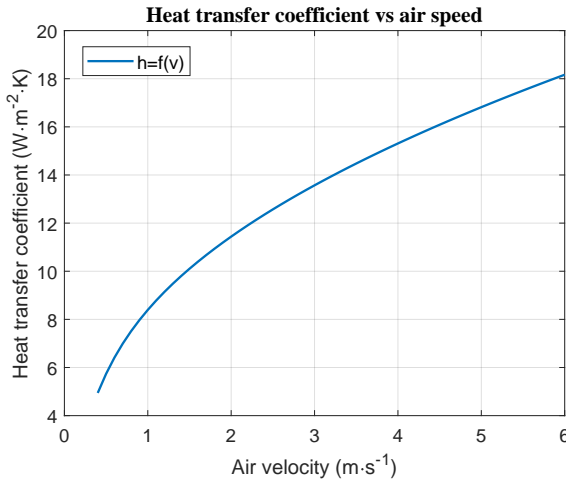


Fig. 13: The calculated dependency of the convection coefficient.

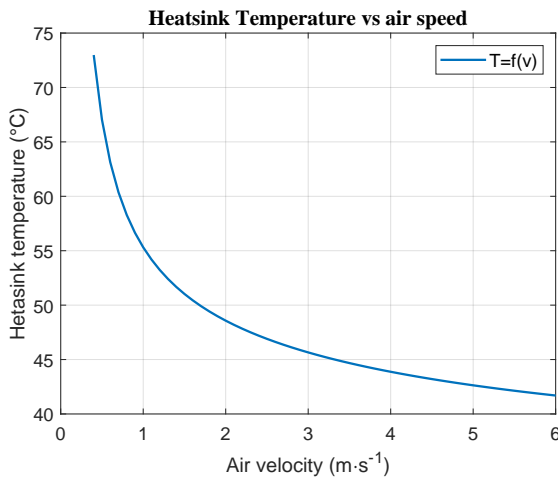


Fig. 14: Heatsink temperature vs. air velocity.

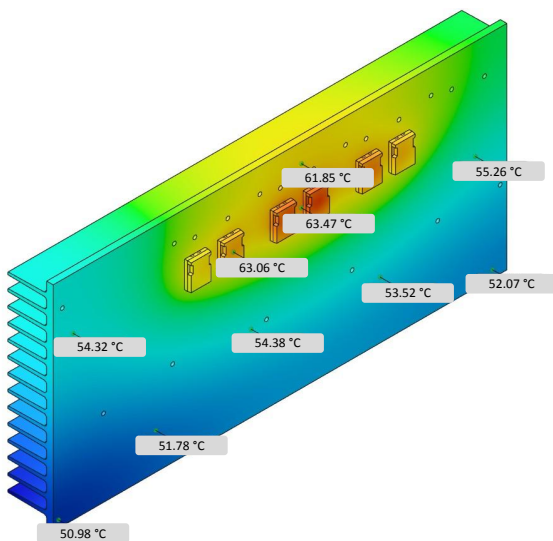


Fig. 15: Simulated results at air velocity 1 m.s⁻¹ - convection only.

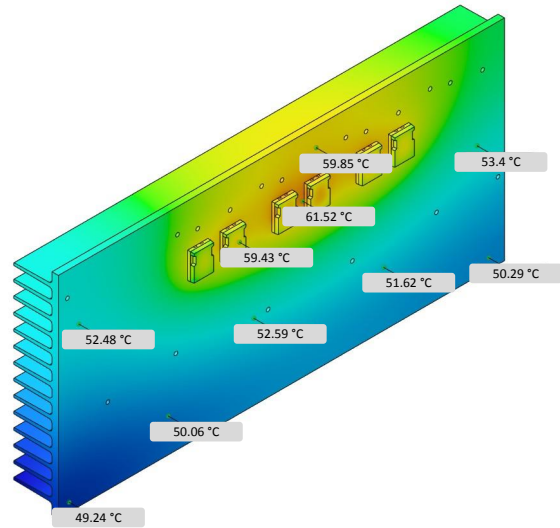


Fig. 16: Simulated results at air velocity 1 m.s⁻¹ - convection and radiation.

5. Discussion

The difference between the proposed methods is that the first-mentioned one needs the value of heatsink thermal resistance for temperature calculation. The other method (Fusion 360) uses the geometry of the heatsink, the estimated power losses, and the convection coefficient to simulate heat spreading. The worst-case scenario losses were estimated to be 87 W, and this value was used to estimating the heat spreading of the heatsink.

The MATLAB simulation considers only convection for temperature calculation as well as the iterative method. The Fusion 360 can utilize both the convection and radiation. By comparing Fig. 7 and Fig. 11, we can see that the calculated (76 °C) and visualized (75.8 °C) temperatures of the heatsink are nearly the same. The same results occur for the junction and case temperature. It should be noted that the mentioned results are for the convection analysis. The convection coefficient was calculated with the use of the heat transfer formula [19] and iterative method as well, Fig. 9. This coefficient includes heatsink dimensions and no forced airflow, only natural convection. The simulation in Fusion 360 then shows heat spreading in the heatsink, Fig. 11. Another simulation includes radiation in addition to convection, Fig. 12.

If forced airflow is required, Eq. (2), Eq. (3), Eq. (4) and Eq. (5) were used to calculate the heat transfer coefficient at different airflows. The results are shown in Fig. 13. According to Fig. 14, the steady-state temperature of the heatsink can be designed depending on the air velocity. The value of the heat transfer coefficient can be then used to visualize heat spreading at differ-

ent air velocity in Fusion 360. In case the convection and radiation are considered, the average temperature is 52.9 °C, as shown in Fig. 16.

Therefore, if the natural convection is used, the MATLAB method is satisfactory for the fast design of the heatsink. If the forced cooling is required, the MATLAB method is complemented by the finite element method using Fusion 360 and the iteration method. It must be said that the presented model can be used for any converter and any transistors. However, the converter topology must be modified, and the characteristics of the transistor must be specified.

6. Conclusion

This paper discusses IGBT power loss estimation in three-phase inverter using the simulation method in MATLAB Simulink. The main advantage of this method is fast loss estimation, where different IGBT models can be added fast. The model calculates all losses, switching and conducting in transistor and internal diode too. Based on this, the power loss of the three-phase inverter at different working conditions was investigated. The main goal of this investigation was the worst-case scenario loss estimation. For this aim, the parametric simulation was used. The highest losses were at the lowest RPM and highest simulated torque, because of low BEMF and high inverter currents. The selected heatsink is capable of the inverter cooling in the worst-case scenario, but forced airflow is needed to ensure that the semiconductors will have lower temperatures, which can improve lifetime and reliability.

The proposed MATLAB Simulink method is a fast way to determine losses in different converters topologies because the model can be reconfigured to the required topology as well as calculating the heatsink, case, and junction temperature. The design of the heatsink using Fusion 360 software is a tool to visualize the temperature, but the value of the convection coefficient must be known. The comparison of the two methods gives a good match of results, and therefore, the proposed method can be used as a basis in the design of power converters and its cooling solutions.

Acknowledgment

This work was supported by projects: KEGA project no. 027ZU-4/2018, APVV-15-0571: Research of the optimum energy flow control in the electric vehicle system, ITMS 26220220078 - Research of high effective components of electric drive systems of urban electric vehicles.

References

- [1] PRAZENICA, M., J. KASSA and J. SEDLAK. Investigation of Power Losses of Two-Stage Two-Phase Converter with Two-Phase Motor. *Advances in Electrical and Electronic Engineering*. 2011, vol. 9, iss. 2, pp. 77–83. ISSN 1804-3119. DOI: 10.15598/aeec.v9i2.503.
- [2] SPANIK, P., B. DOBRUCKY, M. FRIVALDSKY, P. DRGONA and I. LOKSENINEC. Experimental Analysis of Commutation Process of Power Semiconductor Transistor's Structures. *Advances in Electrical and Electronic Engineering*. 2007, vol. 6, iss. 1, pp. 50–53. ISSN 1804-3119.
- [3] SENTURK, O. S., S. MUNK-NIELSEN, R. TEODORESCU, L. HELLE and P. RODRIGUEZ. Electro-thermal modeling for junction temperature cycling-based lifetime prediction of a press-pack IGBT 3L-NPC-VSC applied to large wind turbines. In: *IEEE Energy Conversion Congress and Exposition*. Phoenix: IEEE, 2011, pp. 568–575. ISBN 978-1-4577-0542-7. DOI: 10.1109/ECCE.2011.6063820.
- [4] ZHOU, Z., P. M. HOLLAND and P. IGIC. Compact thermal model of a three-phase IGBT inverter power module. In: *26th International Conference on Microelectronics*. Nis: IEEE, 2008, pp. 167–170. ISBN 978-1-4244-1881-7. DOI: 10.1109/ICMEL.2008.4559249.
- [5] ZELNIK, R. and M. PRAZENICA. Multiple Output Flyback Converter Design. *Transactions on Electrical Engineering*. 2020, vol. 8, iss. 3, pp. 32–39. ISSN 1805-3386. DOI: 10.14311/TEE.2019.3.032.
- [6] ANTONIOS, J., N. GINOT, C. BATARD, Y. SCUDELLER and M. MACHMOUM. Electro-thermal investigations on silicon inverters operating at low frequency. In: *11th International Thermal, Mechanical & Multi-Physics Simulation, and Experiments in Microelectronics and Microsystems (EuroSimE)*. Bordeaux: IEEE, 2010, pp. 1–5. ISBN 978-1-4244-7026-6. DOI: 10.1109/ESIME.2010.5464511.
- [7] CUBON, P., J. SEDO, R. RADVAN, J. STANCEK, P. SPANIK and J. URICEK. Calculation of demand of electric power of small electric vehicle using Matlab GUI. In: *ELEKTRO*. Rajecke Teplice: IEEE, 2014, pp. 149–153. ISBN 978-1-4799-3721-9. DOI: 10.1109/ELEKTRO.2014.6847891.
- [8] OVANDO, R. B. B., F. A. RAMIREZ, C. HERNANDEZ and M. A. ARJONA. A 2D Fi-

- nite Element Thermal Model of a Three-Phase-Inverter Heat Sink. In: *IEEE Electronics, Robotics and Automotive Mechanics Conference*. Morelos: IEEE, 2010, pp. 696–701. ISBN 978-1-4244-8149-1. DOI: 10.1109/CERMA.2010.141.
- [9] SPANIK, P., J. CUNTALA, M. FRIVALDSKY and P. DRGONA. Investigation of Heat Transfer of Electronic System through Utilization of Novel Computation Algorithms. *Electronics and Electrical Engineering*. 2012, vol. 123, iss. 7, pp. 31–36. ISSN 2029-5731. DOI: 10.5755/j01.eee.123.7.2371.
- [10] FRIVALDSKY, M., P. SPANIK, P. DRGONA and Z. LONCOVA. Algorithms for indirect investigation of heat distribution in electronic systems. *International Journal of Thermal Sciences*. 2017, vol. 114, iss. 1, pp. 15–34. ISSN 1290-0729. DOI: 10.1016/j.ijthermalsci.2016.12.005.
- [11] SPANIK, P., B. DOBRUCKY and M. FRIVALDSKY. Measurement of switching losses in power transistor structure. *ELEKTRONIKA IR ELEKTROTECHNIKA*. 2008, vol. 82, iss. 2, pp. 75–78. ISSN 1392-1215.
- [12] PASKALA, M., M. PRIDALA, M. PIPISKA and P. HUDAK. The support system for testing the power converters: The system of water cooling / heating. In: *ELEKTRO*. Strbske Pleso: IEEE, 2016, pp. 196–200. ISBN 978-1-4673-8698-2. DOI: 10.1109/ELEKTRO.2016.7512064.
- [13] CASANELLAS, F. Losses in PWM inverters using IGBTs. *Electric Power Applications*. 1994, vol. 141, iss. 5, pp. 235–239. ISSN 1751-8660.
- [14] BIERHOFF, M. H. and F. W. FUCHS. Semiconductor losses in voltage source and current source IGBT converters based on analytical derivation. In: *IEEE 35th Annual Power Electronics Specialists Conference (IEEE Cat. No.04CH37551)*. Aachen: IEEE, 2004, pp. 2836–2842. ISBN 0-7803-8399-0. DOI: 10.1109/PESC.2004.1355283.
- [15] KHOSHKBAR S. A., V. DARGAHI and K. CORZINE. Calculation of conduction power losses in double flying capacitor multicell converter. In: *IEEE Applied Power Electronics Conference and Exposition (APEC)*. Charlotte: IEEE, 2015, pp. 2351–2357. ISBN 978-1-4799-6735-3. DOI: 10.1109/APEC.2015.7104677.
- [16] DYBKO, M. A., S. S. TURNAEV and S. V. BROVANOV. A power losses calculation in a four-legged three-level voltage source inverter. In: *International Conference and Seminar on Micro/Nanotechnologies and Electron Devices*. Novosibirsk: IEEE, 2009, pp. 365–369. ISBN 978-1-4244-4571-4. DOI: 10.1109/EDM.2009.5174013.
- [17] 7th Generation IGBT Module T/T1 – Series Application Note. In: *MITSUBISHI ELECTRIC CORPORATION* [online]. 2018. Available at: http://www.mitsubishielectric.com/semiconductors/files/manuals/igbt_t_note_e.pdf.
- [18] ROETZEL, W. Iteration-free calculation of heat transfer coefficients in heat exchangers. *The Chemical Engineering Journal*. 1977, vol. 13, iss. 2, pp. 233–237. ISSN 1385-8947. DOI: 10.1016/0300-9467(77)80078-6.
- [19] TEERTSTRA, P., M. M. YOVANOVICH, J. R. CULHAM and T. LEMCZYK. Analytical forced convection modeling of plate fin heat sinks. In: *Fifteenth Annual IEEE Semiconductor Thermal Measurement and Management Symposium (Cat. No.99CH36306)*. San Diego: IEEE, 1999, pp. 34–41. ISBN 0-7803-5264-5. DOI: 10.1109/STHERM.1999.762426.
- [20] HLADKY, V. and R. BIELEK. Modelling and Control of Thermal System. *Advances in Electrical and Electronic Engineering*. 2014, vol. 12, iss. 2, pp. 103–110. ISSN 1804-3119. DOI: 10.15598/aeec.v12i2.921.

About Authors

Patrik RESUTIK was born in 1995 in Trstena Slovak Republic. He is a Ph.D. student at University of Zilina, Faculty of Electrical Engineering and Information Technology – Department of Mechatronics and Electronics in the study programme “Power Electronics”. His research interests include switching mode power supply and matrix converter design.

Slavomir KASCAK was born in Krompachy, Slovak Republic. He received the M.Sc. degree in power electronics and the D.Sc. degree in automation focused on electrical drives from the Faculty of Electrical Engineering of the University of Zilina, Slovak Republic, in 2010 and 2013, respectively. He is currently a Researcher and an Assistant Professor in Department of Mechatronics and Electronics. His current research activities include power electronics, electrical drives, and control.